Shrink film patterning by craft cutter: complete plastic chips with high resolution/high-aspect ratio channel†‡

Douglas Taylor, David Dyer, Valerie Lew and Michelle Khine*

Received 29th March 2010, Accepted 21st June 2010
DOI: 10.1039/c004737f

This paper presents a rapid, ultra-low-cost approach to fabricate microfluidic devices using a polyolefin shrink film and a digital craft cutter. The shrinking process (with a 95% reduction in area) results in relatively uniform and consistent microfluidic channels with smooth surfaces, vertical sidewalls, and high aspect ratio channels with lateral resolutions well beyond the tool used to cut them. The thermal bonding of the layers results in strongly bonded devices. Complex microfluidic designs are easily designed on the fly and protein assays are also readily integrated into the device. Full device characterization including channel consistency, optical properties, and bonding strength are assessed in this technical note.

Introduction

For microfluidic technology to make a significant impact on promising applications including cell culture,[1,2] modeling of cell–cell interactions,[3] systems biology,[4] and point-of-care diagnostics,[5,6] the persistent chasm between academic prototyping and industry-standard devices must be bridged. While most academic labs prototype *via* soft lithography in polydimethylsiloxane (PDMS), industry is typically intolerant to its significant drawbacks, including swelling, non-selective absorption, and poor mechanical properties. Instead, industry relies on plastics, including polystyrene (PS) and polyolefins (PO).[7] To create such fine features in plastics typically requires either hot embossing or injection molding; both approaches require expensive capital equipment and extensive processing time that largely precludes academic prototyping.[8,9] While laser ablation is a promising new, more economical approach, interactions between the laser light and the polymer can induce unwanted surface modifications and are limited in resolution to the spot size of the laser.[9–11]

The use of laminated polymers to form stacked layers that ultimately define the components of a microfluidic chip offers several advantages to hot embossing, injection molding, laser ablation, and casting. These advantages include time of fabrication, reproducibility, low-cost, and strong, biocompatible bonds between layers.[12] However, the use of adhesives to bond the different layers introduces material into the side-walls of the channels that are often inhomogeneous to the properties of the bulk material.[13] The cutting of channels into the substrate layers often employs the use of a laser, which substantially increases the expense of such a fabrication technique.[14] In a recent work, the fabrication of polymer laminate-based microfluidic devices with a digital craft cutter was explored as a low-cost alternative to the use of a laser.[15] The channel resolutions achieved with the craft cutter were, however, limited.[15] The use of shrink polymeric films would circumvent this limitation by allowing one to achieve channel resolutions beyond the limits of the fabrication machinery.

Previous works with shrink films have focused on the applications of a polystyrene toy called "Shrinky-Dinks".[16] PS was shown to display a 60% reduction in area upon shrinkage and was used in conjunction with a laser printer to fabricate masters for the fabrication of PDMS microfluidic devices and micro wells.[16,17] Direct patterning of the sheets through etching or deposition was shown to create complete microfluidic devices, and was expanded upon to create a functional biochip that integrated a complex microfluidic design and proteins spots.[18–20] Recently, a shrink material comprised of PO was characterized to exhibit a 95% reduction in area for high-aspect ratio templates for soft lithography.[21]

This paper presents a novel, rapid, ultra-low-cost strategy to fabricate microfluidic devices capable of integrating functional immunoassays utilizing PO shrink film and a digital craft cutter. The shrinking process results in relatively uniform and consistent microfluidic channels with smooth surfaces, vertical sidewalls, and high aspect ratio channels with lateral resolutions well beyond the tool used to cut them. The thermal bonding of the layers results in a strongly bonded chip, with leak proof channels, and homogenous surface and bulk properties. Complex microfluidic designs can be easily designed on the fly and protein assays also readily integrated into the device.

Methods and materials

Fabrication of the device

PO shrink film (Sealed Air Nexcel multilayer shrink film 955D) of a 1 mil (0.0254 mm) thickness composed of 5 layers of co-extruded PO was laminated to a polyester backing of a 3 mil (0.0762 mm) thickness as previously described.[21]

A digital craft cutter (Quickutz Silhouette SD) was employed for the through cutting of all channels.[15] The corners and edges of the substrate were taped to the backing to ensure that the substrate did not move, remained flat, and that the shrink film could not be peeled off its laminated backing during the cutting

Department of Biomedical Engineering, University of California, Irvine, CA, USA. E-mail: mkhine@uci.edu

† Published as part of a special issue dedicated to Emerging Investigators: Guest Editors: Aaron Wheeler and Amy Herr.

‡ Electronic supplementary information (ESI) available: Optical data (transmission and autofluorescence measurements). See DOI: 10.1039/c004737f

process. Channels could be designed in the Craft Robo software (Graphtec Robo Master) or in a CAD software (AutoCAD®) and loaded into the Craft Robo Controller as a.DXF file. The latter method was chosen in order to achieve greater control over the accuracy and precision of the designed channels.

The through-cut layers of the microfluidic device were removed from the backing (Fig. 1a and b). The through-cut layers were arranged and aligned using 0.4 mm diameter pins (Clover® Patchwork Pins Fine) (Fig. 1c). The aligned layers and pins were placed on a 4 in. diameter silicon wafer and placed in a cool oven. The sample was heated in a step-wise fashion as follows: the oven was heated to 115 °C and held for approximately 5 minutes, then heated to 135 °C and held for approximately 5 minutes, and then heated to 155 °C. At the conclusion of the shrinking process, the silicon wafer and substrate were removed from the oven, and the pins in the chip were removed with tweezers (Fig. 1d). To ensure flatness of the chip, the wafer and substrate were re-inserted to the oven at 155 °C for approximately 20 minutes. Gentle pressure was applied at the chip corners with tweezers to ensure flatness before removal from the oven.

Characterization of device

Channels of variable widths and constant lengths were cut for characterization of the sidewalls and channel width resolutions of the Quickutz silhouette in conjunction with shrinkage. Widths of pre-shrunk dimensions 1.0, 0.6, and 0.2 mm were measured *via* an optical profilometer (The Hyphenated Systems HS200 OP optical profiler) with a confocal microscope (Nikon Eclipse L200).

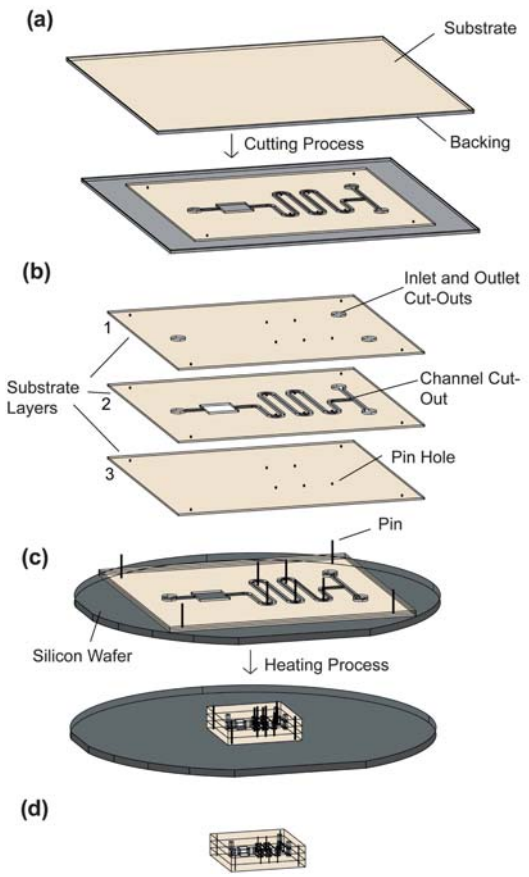

Fig. 1 Fabrication process diagram. (a) Etching of the substrate using a digital craft cutter, (b) removal of the shrink film from its laminate backing and alignment, and (c) shrinking of the substrate to achieve a thermally bonded, shrunk, microfluidic device (d).

Next, five 3-layer channel devices were characterized for channel width homogeneity. The chips consisted of a "T" junction, a mixer region, and an assay region (Fig. 1). All channels except for the assay region were 1 mm in width pre-shrunk. Post-shrinkage, fluorescent dye (Alexa Fluor 555) was injected into the channel and fluorescently imaged on an inverted fluorescence microscope (Olympus IX51&BH2-RFL-T3) and image capture software (QCapture Pro). Three channel images were recorded in the "T" junction region and two in the mixer region from each of the chips for analysis (Fig. 3). Line intensity measurements were taken using ImageJ. The width of the channels was assessed as the distance between the full-width, half-maximum points of the line intensity profiles using MATLAB®.

Immunoassay

A 3-layer microfluidic device was cut as described above. Prior to alignment of the individual substrate, layer 3 was stamped with 100 μg ml^{-1} of primary rabbit IgG (Molecular Probes) dissolved in 50 mM of sodium phosphate buffer solution (pH = 7) by microcontact printing.[22,23] PDMS stamps made from a silicon master were used. Prior to stamping, the PDMS stamps were sonicated (Branson) in 70% ethanol for 10 minutes, 1 molar solution of sodium hydroxide for 10 minutes, and DI water for 10 minutes. The stamps were air dried and exposed to oxygen plasma (SPI Supplies) for 30 seconds to render the surface hydrophilic. The PO substrates were sonicated in DI water for 10 minutes and left to air dry.

After stamping, the substrate was incubated for 4 hours then washed with DI water. The outlined region was incubated with BSA blocking solution to prevent non-specific binding of the secondary anti-bodies for 4 hours, then washed with DI water. The layers were assembled, aligned with pins, and shrunk. 20 μg ml^{-1} of anti-rabbit IgG conjugated with dye (AlexaFluor 555) was injected into the microfluidic device through one of the inlet holes so that the immunoassay region of the device was covered with solution. The device was incubated for 2 hours. The channels were rinsed with DI water by flowing DI water through the channels, and then fluorescently imaged on an inverted microscope.

Results and discussion

Characterization of the device

In order to assess how our shrinking method improved the limit of resolution using Quickutz Silhouette SD, channels of various widths were measured *via* an optical profilometer. Channels of pre-shrunk widths of 1.0, 0.6, and 0.2 mm were characterized as having post-shrunk widths of 211, 128, and 95 μm respectively (Fig. 2a). It was previously assessed that the Quickutz Silhouette's lateral feature resolution was 0.2 mm.[15] Our method of utilizing shrink polymers was able to achieve a significant improvement in lateral feature resolution.

The topographical analysis of the multi-width channels (Fig. 2) depicts near vertical side walls, high aspect ratios, and smooth surface features. The channel walls were on the order of 600 μm for

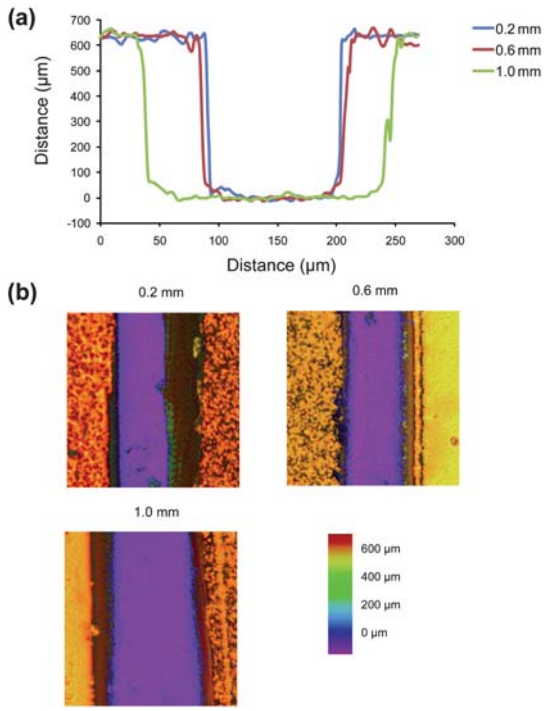

Fig. 2 Channel characterization by optical profilometry. Topographical micrograph of channels depicted in (b) with the pre-shrunk channel widths of 0.2, 0.6, and 1.0 mm labeling lines in (a) and above the image in (b).

all three samples determined by the thickness of the sheet; different thickness sheets can be chosen to meet desired channel heights. Vertical side walls and high aspect ratios have various applications in cell culture[24] and on chip purification for diagnostics,[25] but are difficult to achieve and require costly procedures and expensive equipment.[9,26] This is particularly true when using molds involving elastomeric polymers such as PDMS.

Line intensity profiling (Fig. 3) of the 3-layer chips highlights the decrease in channel size obtained after shrinkage. An average reduction in channel width of 76% and an average variance in channel width of 14% for the five chips tested were recorded. Variances in the channel width can be attributed to non-uniformities arising from the shrinking process. However, it should be noted that no channel blockage or collapse was observed. It will be necessary to optimize the shrink films used and the shrinking process to obtain less variance in channel dimensions. The use of fluorescent dye to image the channel shows that channels are also leak proof (Fig. 3). Pressure testing indicated that the thermal bonding could withstand pressures in excess of 50 psi (ESI‡).

Optical data (transmission and autofluorescence measurements) are available in the ESI‡.

Immunoassay

Fluorescence-based detection is a commonly employed strategy in POC diagnostics.[14] To demonstrate the potential of our fabrication method, a functioning 3-layer, PO microfluidic device with an integrated protein assay (Fig. 4a) was fabricated and tested. Fluorescently labeled anti-bodies were flown through the device where they selectively attached to proteins that had been

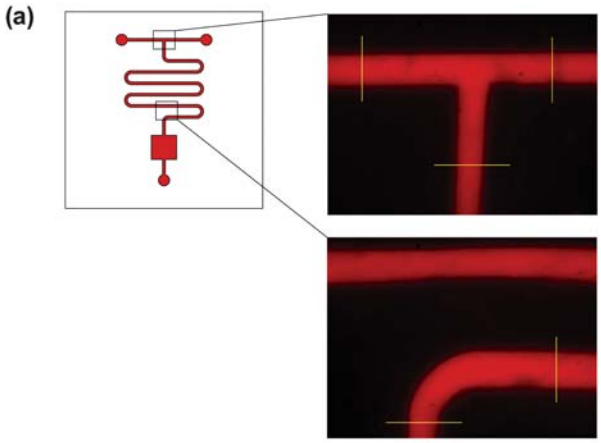

Average Channel Width (μm)	% Reduction	Standard Deviation (μm)	% Channel Width Variance
235	77	34	14

Fig. 3 Channel characterization by line intensity. (a) A schematic of the layout of the device is given with enlarged micrographs of the selected areas taken with fluorescence microscopy (pseudo-colored red). The yellow lines indicate the approximate region where the line intensity profiles were taken. The original width of the channels except the assay region was 1 mm. (b) Summary of channel width characterization.

previously microcontact printed prior to the device assembly and shrinkage. Micrographs (Fig. 4b) depict the array under a TRITC filter viewed through the top of the device (layer 1) to the assay region at the bottom of the device (layer 3).

It was previously demonstrated that proteins stamped onto PS are functional even after exposure to high temperatures and

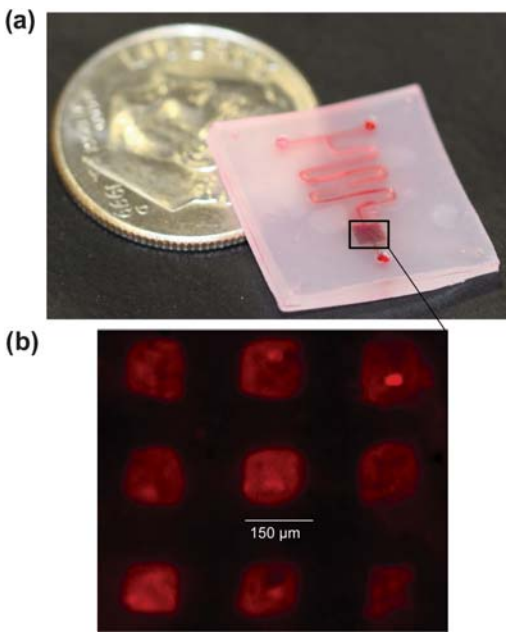

Fig. 4 Immunoassay. (a) Fluorescently labeled anti-rabbit IgG was pipetted through the microfluidic device where it selectively bound to the primary rabbit IgG deposited in the array region of the device, which is outlined in black. (b) Micrographs of the fluorescently-labeled array of protein spots in (a) were taken at 4× (pseudo colored-red).

enhance the sensitivity of the assay due to increased density of the deposited proteins after shrinkage. This results in higher fluorescence intensity, and greater homogeneity of the deposited proteins after shrinkage.[18] This was also demonstrated using PO.[21] It should be noted, however, that a complete microfluidic device entirely composed of shrink polymers with an integrated protein assay has not been achieved until now.

Conclusion

A functional microfluidic immunoassay device fabricated out of PO shrink film was described. The use of multiple thin film substrates to compose a device layer by layer allows one to achieve vertical side walls and smooth channel surfaces as well as allows one to control the height of the channels by selecting the thickness of the film. The shrinkage process maintains the spatial homogeneity of the channel dimensions while decreasing the channel width and increasing the channel height. Thermal bonding of the substrates produces leak-proof channels that have the same properties as those of the bulk material. While the optical properties of the material used to fabricate the device post-shrinkage proved to deviate from the ideal, the problems of opacity and autofluorescence do not inhibit the device from being used in conjunction with fluorescence microscopy. A fully functioning immunoassay was also integrated into the device.

Acknowledgements

This work was supported by Shrink Nanotechnologies and MF3 at UC Irvine.

References

1 K. J. Jang and K. Y. Suh, *Lab Chip*, 2010, **10**, 36–42.
2 J. H. Yeon and J. K. Park, *Biochip. J.*, 2007, **1**, 17–27.
3 M. Antia, T. Herricks and P. K. Rathod, *PLoS Pathog.*, 2007, **3**, 939–948.
4 T. Danino, O. Mondragon-Palomino, L. Tsimring and J. Hasty, *Nature*, 2010, **463**, 326–330.
5 H. Y. Tan, W. K. Loke, Y. T. Tan and N. T. Nguyen, *Lab Chip*, 2008, **8**, 885–891.
6 L. Gervais and E. Delamarche, *Lab Chip*, 2009, **9**, 3330–3337.
7 C. K. Fredrickson, Z. Xia, C. Das, R. Ferguson, F. T. Tavares and Z. H. Fan, *J. Microelectromech. Syst.*, 2006, **15**, 1060–1068.
8 P. Abgrall, L. N. Low and N. T. Nguyen, *Lab Chip*, 2007, **7**, 520–522.
9 H. B. Liu and H. Q. Gong, *J. Micromech. Microeng.*, 2009, **19**, 037002.
10 D. Snakenborg, H. Klank and J. P. Kutter, *J. Micromech. Microeng.*, 2004, **14**, 182–189.
11 B. Li, T. Schwarz and A. Sharon, *J. Micromech. Microeng.*, 2006, **16**, 2639–2645.
12 P. M. Martin, D. W. Matson, W. D. Bennett, Y. Lin and D. J. Hammerstrom, *J. Vac. Sci. Technol., A*, 1999, **17**, 2264–2269.
13 D. Paul, A. Pallandre, S. Miserere, J. Weber and J. L. Viovy, *Electrophoresis*, 2007, **28**, 1115–1122.
14 R. Irawan, T. S. Chuan and F. C. Yaw, *Microwave Opt. Technol. Lett.*, 2005, **45**, 456–460.
15 P. K. Yuen and V. N. Goral, *Lab Chip*, 2010, **10**, 384–387.
16 A. Grimes, D. N. Breslauer, M. Long, J. Pegan, L. P. Lee and M. Khine, *Lab Chip*, 2008, **8**, 170–172.
17 D. Nguyen, S. Sa, J. D. Pegan, B. Rich, G. X. Xiang, K. E. McCloskey, J. O. Manilay and M. Khine, *Lab Chip*, 2009, **9**, 3338–3344.
18 K. Sollier, C. A. Mandon, K. A. Heyries, L. J. Blum and C. A. Marquette, *Lab Chip*, 2009, **9**, 3489–3494.
19 M. Long, M. A. Sprague, A. A. Grimes, B. D. Rich and M. Khine, *Appl. Phys. Lett.*, 2009, **94**, 133501.
20 C. S. Chen, D. N. Breslauer, J. I. Luna, A. Grimes, W. C. Chin, L. P. Leeb and M. Khine, *Lab Chip*, 2008, **8**, 622–624.
21 D. Nguyen, D. Taylor, K. Qian, N. Norouzi, J. Rasmussen, S. Botzet, K. H. Lehmann, K. Halverson and M. Khine, *Lab Chip*, 2010, **10**, 1623–1626.
22 D. Qin, Y. N. Xia and G. M. Whitesides, *Nat. Protocols*, 2010, **5**, 491–502.
23 K. E. Schmalenberg, H. M. Buettner and K. E. Uhrich, *Biomaterials*, 2004, **25**, 1851–1857.
24 P. J. Hung, P. J. Lee, P. Sabounchi, N. Aghdam, R. Lin and L. P. Lee, *Lab Chip*, 2005, **5**, 44–48.
25 J. Wen, L. A. Legendre, J. M. Bienvenue and J. P. Landers, *Anal. Chem.*, 2008, **80**, 6472–6479.
26 U. Stohr, P. Vulto, P. Hoppe, G. Urban and H. Reinecke, *J. Micro/ Nanolithogr., MEMS, and MOEMS*, 2008, **7**, 033009.